Journal of Solid State Chemistry 182 (2009) 1661–1665

Contents lists available at ScienceDirect

Journal of Solid State Chemistry

journal homepage: www.elsevier.com/locate/jssc

Fabrication of $Cs_{2.5}H_{0.5}PW_{12}O_{40}$ three-dimensional ordered film by colloidal crystal template

Fang Chai [a,b], Dongliu Li [a], Hongbo Wu [a,b], Chunli Zhang [a], Xiaohong Wang [a,*]

[a] Key Lab of Polyoxometalate Science of Minister of Education, Northeast Normal University, Changchun 130024, PR China
[b] Department of Chemistry, Harbin Normal University, Harbin 150500, PR China

ARTICLE INFO

Article history:
Received 25 November 2008
Received in revised form
19 March 2009
Accepted 28 March 2009
Available online 9 April 2009

Keywords:
Polyoxometalate
Colloidal crystal
Template
Photonic band gap

ABSTRACT

A three-dimensional ordered polyoxometalate periodic film was synthesized using dodecatungstophosphoric acid ($H_3PW_{12}O_{40}$) and Cs_2CO_3 as precursors and colloidal crystals as templates by an inverse opal method. The samples were characterized by elemental analysis, XRD, IR spectra, UV–Vis diffuse reflectance spectra (DR–UV–Vis) and SEM techniques. This arrayed film constructed by pure cesium salt of dodecatungstophosphoric acid $Cs_{2.5}H_{0.5}PW_{12}O_{40}$ nanoparticles shows well-defined lamellar array with inverse opal structure, which exhibits a well-defined photonic band gap.

1. Introduction

The fabrication of miniature objects by particles self-assembly into colloidal crystals with various morphologies has attracted widespread interest because of the objects' inherent nanoscale optical, electrical, magnetic, and catalytic functionality [1–5]. Monodisperse colloids (e.g. silica and polystyrene (PS) microspheres) spontaneously organize under certain conditions to form three dimension (3D) face-centered cubic (fcc) lattices on solid substrates [6–8] or on microbeads [9]. These planar crystals exhibit a periodic spatial variation of refractive index with lattice constants on the order of the wavelength of light, thus exhibiting a well-defined photonic band gap (PBG) [10,11]. These colloidal crystals (opal) can provide templates in creating periodic nanostructures, in which some desired precursors such as liquid metal alkoxides [12,13], nanoparticle [14] solutions (carbonate, oxalate, acetate solution) [15,16] are filled and are solidified *in situ* via a sol–gel transformation. Ordered foams (inverse opals) are produced after removing the template by calcinations or extraction. Compared with the silicon alkoxides, the hydrolysis and polymerization of transition-metal alkoxides are more difficult to control. 'Nanocasting' approach by Ryoo [17] is an efficient way to restrict the formation and growth of metal and metal oxide species using simple metal salts as precursors.

Polyoxometalate (POMs), a kind of well-known metal-oxide nanoclusters with unique variety in size, composition, and function, are attracting increasing attention in areas of catalysis [18], magnetism [19], photoluminescence [20–23], photochromism [24] and proton conduction for fuel cells [25]. However, the application of these inorganic clusters in thin film device still remains a challenge due to the poor processibility of inorganic crystalline solids, which retards the value-adding properties of POMs for materials [26]. Compared to the rapid increase of new structures, the fabrication of the functional POMs materials has increased slowly. Therefore, the development of suitable methods and technologies to utilize POMs has became a focus topic in POMs chemistry [27]. In the past, the array films based on POMs clusters are made by the Langmuir-Blodgett technique [28], and the soft lithographic approach using cationic surfactants [29–32]. As we all known, polyoxometalates are soluble in water and some polar solvents. Therefore, it is difficult to fabricate 3D thin film simply by POMs anions as precursors being filled within colloidal crystal templates. POMs anions which infiltrate into the voids of colloidal crystal templates could not form stable self-supported structure. Because when the templates are removed, the porous structures will collapse completely. Combination of 'inverse opals' and the 'nanocasting' approaches can provide an available method to infiltrate POMs into the voids of the colloidal crystals and solidify them as cesium salts by the reacting of POMs anions with cesium cations in the voids. It has been reported [33] that dodecatungstophosphoric acid reacted with Cs_2CO_3 to form polyoxometallic nanoparticles in formula $Cs_xH_{3-x}PW_{12}O_{40}$, which might be used as a precursor to fabricate 3D POMs ordered thin film.

* Corresponding author. Fax: +86 431 85099759.
E-mail address: Wangxh665@nenu.edu.cn (X. Wang).

0022-4596/$ - see front matter © 2009 Elsevier Inc. All rights reserved.
doi:10.1016/j.jssc.2009.03.035

We now report a general method to prepare self-supported $Cs_{2.5}H_{0.5}PW_{12}O_{40}$ 3D ordered array film via combination of 'inverse opal' and 'nanocasting' route by coprecipitation of Cs^+ and $PW_{12}O_{40}^{3-}$ *in situ*, which takes place in the interstices of the polystyrene colloidal crystals and involves successive filtration. This arrayed film is constructed by cesium salt of dodecatungstophosphoric acid showing well-defined lamellar array with inverse opal structure, which exhibits a well-defined photonic band gap (PBG).

2. Experimental

2.1. Materials

All chemicals, Cs_2CO_3, styrene and $H_3PW_{12}O_{40}$ are of analytical grade and used without further purification. PS microspheres with diameters of about 660 nm were synthesized by the emulsion polymerization method, and PS colloidal crystal template with ordered opal structure assembled on glass, quartz and silicon substrate by vertical deposit technique [34].

2.2. Synthesis

Two stock solutions of 0.003 M of Cs_2CO_3 and 0.0012 M of $H_3PW_{12}O_{40}$ have been prepared at room temperature. In the first step, a piece of PS template was soaked in the solution of Cs_2CO_3 for about 30 min. Secondly, the solution of $H_3PW_{12}O_{40}$ was added dropwise to the above template in a Büchner funnel while suction was applied. Then these two solutions were filtered for some times by turns, in which the deposition of $Cs_xH_{3-x}PW_{12}O_{40}$ was produced by the reaction between Cs^+ and $PW_{12}O_{40}^{3-}$ as soon as two solutions mixed, where x corresponds to the filling times. The above two steps were repeated for about 10, 15, 20, 25 times to find the most appropriate condition. Finally the voids of template were filled with precipitation of $Cs_xH_{3-x}PW_{12}O_{40}$. The sample was washed two times with distilled water to remove the superfluous deposition. Then the as-prepared material containing $PS/Cs_xH_{3-x}PW_{12}O_{40}$ was dried by airflow, and then was extracted by a solution of tetrahydrofuran/acetone (1:1) to remove the PS template. Thus, the $Cs_xH_{3-x}PW_{12}O_{40}$ 3D ordered thin film was prepared with yield 30%. The yield of 3D POM thin film can be obtained by weight.

2.3. Characterization

Elemental analyses of the films were carried out using a Leeman Plasma Spec (I) ICP-ES. The infrared spectra (IR) (4000–400 cm^{-1}, KBr) of the silicon supported films were recorded by a Nicolet Magna 560 IR spectrometer. UV–Vis absorption spectra of quartz-supported films were recorded on a 756CRT UV–Vis spectrophotometer. Transmittance spectrum of quartz-supported film was recorded on a Varian Cary 500 UV–Vis–NIR Spectrophotometer. The X-ray powder diffraction (XRD) patterns of the samples were collected on a Japan Rigaku D/max 2500 PC X-ray diffractometer equipped with graphite monochromatized Cu$K\alpha$ radiation 40 kV/40 mA ($\lambda = 0.15406$ nm). The morphologies of thin films were imaged with a Hitachi S570 scanning electron microscope (SEM) at 200 kV and a JEOLFESEM 6700F field emission scanning electron microscope with primary electron energy of 3 kV.

3. Results and discussion

In our previous report [35], the silica sol containing POMs was used as a precursor to added into the voids of PS colloidal crystal templates. We attempted to synthesize POMs 3D ordered thin film with honeycomb structure fabricated only by POMs. The successive steps of the impregnation—filtrations for the fabrication of $Cs_xH_{3-x}PW_{12}O_{40}$ are illustrated in Fig. 1. The 'nanocasting' approach is used to fabricate POMs 3D ordered thin film using Cs_2CO_3 and $H_3PW_{12}O_{40}$ as two precursors. Cs_2CO_3 could react with $H_3PW_{12}O_{40}$ to form $Cs_xH_{3-x}PW_{12}O_{40}$ nanoparticles, which is fine particle in common solvents (e.g. water, alcohol, and THF) [36]. The size of $Cs_{2.5}H_{0.5}PW_{12}O_{40}$ was about 10 nm in diameter, which is suitable to fill into the voids of PS templates [36]. The PS colloidal crystals obtained by vertical deposit technique are known to spontaneously self-organize into ordered opal structure with long-range periodicity. After filling of Cs_2CO_3 solution and $H_3PW_{12}O_{40}$ solution alternately, cesium salt of dodecatungstophosphoric acid was precipitated *in situ*. In the meantime, the voids between the spheres were filled, while $Cs_xH_{3-x}PW_{12}O_{40}$ was attached on the PS latex upon drying. The PS template being removed by extracting leaded to a replica of the colloidal crystals, in which $Cs_xH_{3-x}PW_{12}O_{40}$ array film was formed and solidified by sacrificing the PS template.

In the preparation process, one of the most important parameters in creating ordered films is the filling times of the precursors, and experiments were performed for about 10, 15, 20, 25 times, respectively. From the Fig. 2a, it can be seen that the film was not symmetrical after filling 10 times. Fig. 2b shows the surface of film constructed with regular spherical pores array. The wall of the pores was composed of $Cs_xH_{3-x}PW_{12}O_{40}$. When the PS template was filled for more than 20 times (Fig. 2c, d) by the precursor solutions, the edges of pores became thick and crowded. The pores were obviously smaller compared to the above films, and the $Cs_xH_{3-x}PW_{12}O_{40}$ accumulation at the edges can be clearly observed. In order to obtain a fine ordered film, the appropriate times of infiltration of precursor solutions is 15. And it is obvious that the hard template restricts the formation and growth of polyoxometalates by the quantity of precursors [36]. Selection of different size templates can generate different pore size thin film materials.

The contents of Cs^+ and $PW_{12}O_{40}^{3-}$ in film being soaked 15 times were characterized by ICP-AES, which were W, 66.70%, P, 1.03%, Cs, 9.76%, respectively. The molar ratio of P:W:Cs is about 1:12:2.5, indicating that the $Cs_{2.5}H_{0.5}PW_{12}O_{40}$ was formed during filtrating film for 15 times (estimates of errors for analytical data is $<0.5\%$). The contents of Cs^+ and $PW_{12}O_{40}^{3-}$ in film being filtrated 25 times were W, 66.10%, P, 0.94%, Cs, 12.22%, respectively. The molar ratio of P:W:Cs is 1:12:3, indicating that the $Cs_3PW_{12}O_{40}$ was formed during synthetic process for about 25 times. So the filling times

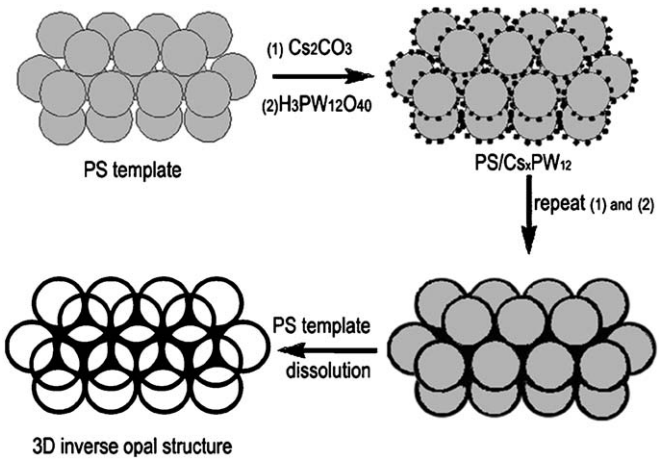

Fig. 1. Schematic illustration of the successive steps for the fabricating $Cs_xH_{3-x}PW_{12}O_{40}$ inverse opal thin film by a PS colloidal crystal template.

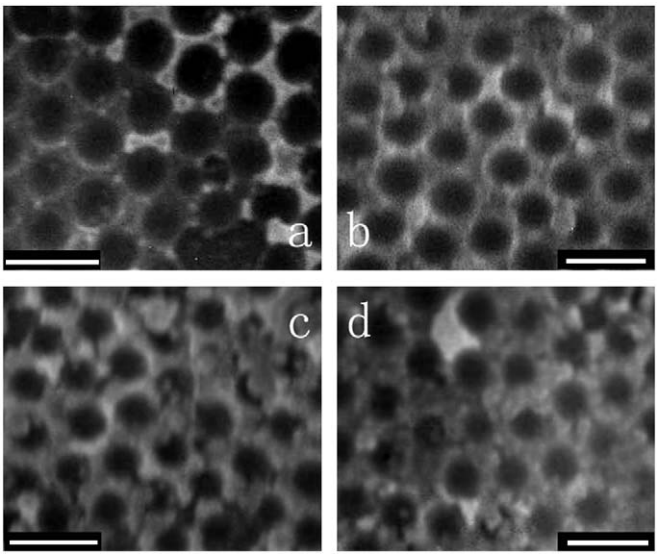

Fig. 2. The SEM images of $Cs_xH_{3-x}PW_{12}O_{40}$ films with different filling times (a. 10, b. 15, c. 20, d. 25, the scale bars are all 1 μm).

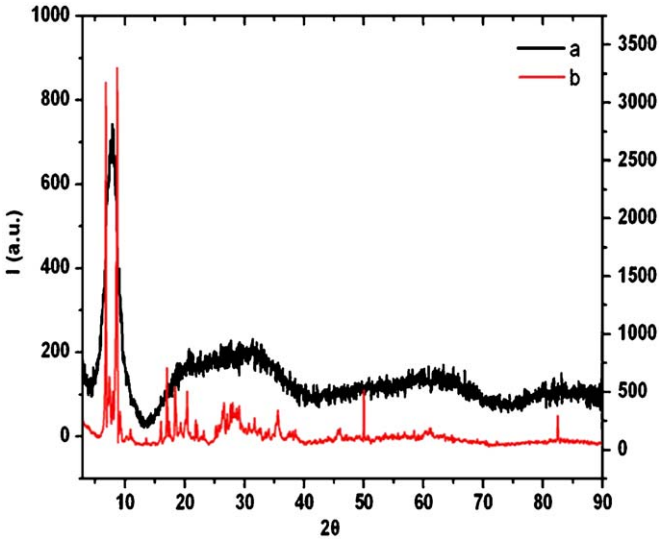

Fig. 3. (a) XRD patterns of $Cs_{2.5}H_{0.5}PW_{12}O_{40}$ thin film and (b) standard (70-0705).

can not only control the formation of the array film but also the components of the film.

The IR spectrum of the $Cs_{2.5}H_{0.5}PW_{12}O_{40}$ array thin film (Supporting Fig. 1) was in good agreement with that of solid $Cs_{2.5}H_{0.5}PW_{12}O_{40}$ observed in macro-scale, with the four characteristic peaks reflected the different vibrations of oxygen atoms of the Keggin-type structure $PW_{12}O_{40}^{3-}$: 1080, 978, 897 and 816 cm^{-1} could be attributed to the asymmetry vibrations P–O_a (internal oxygen connecting P and W), W–O_d (terminal oxygen bonding to W atom), W–O_b (edge-sharing oxygen connecting W) and W–O_c (corner-sharing oxygen connecting W_3O_{13} units). This result shows that the 3D ordered film was constructed by pure dodecatungstophosphoric cesium salts. And the characteristic peaks of PS did not appear in IR spectrum.

UV–Vis spectrum (Supporting Fig. 2) of $Cs_{2.5}H_{0.5}PW_{12}O_{40}$ film fabricated on quart substrate exhibited intense two absorptions at 200 and 269 nm, respectively. The first peak is assigned to the Od→W charge transfer and the second is attributed to the Ob/Oc→W charge transition, which are the two characteristic bands of Keggin heteropolytungstate. This result indicates that the film is fabricated by the primary Keggin structure polyoxometalate and is stable.

The XRD pattern of $Cs_{2.5}H_{0.5}PW_{12}O_{40}$ thin film is shown in Fig. 3a. The three broad reflections appearing at $2\theta = 7.89^\circ$, 27.48° and 61.27° are known to represent poorly crystalline $Cs_{2.5}H_{0.5}PW_{12}O_{40}$ salt compared with the standard $H_3PW_{12}O_{40}$ pattern (70-0705) (Fig. 3b.) This result indicates that the component of POMs is $Cs_{2.5}H_{0.5}PW_{12}O_{40}$ and the POMs in film kept the original Keggin structure [37].

The scanning electron microscopy image was measured to confirm the structure of the film. Fig. 4 shows the SEM images of PS colloidal crystal template and $Cs_{2.5}H_{0.5}PW_{12}O_{40}$ thin film with symmetrical large area 3D periodic structure. It can be seen that the porous structure of film (Fig. 4b) is the exact inverse replicas of the opal colloidal crystals (Fig. 4a) in a large area. Fig. 4b shows the $Cs_{2.5}H_{0.5}PW_{12}O_{40}$ film has inverse opal structure, which is a 3D macroporous structure that comprises highly ordered air spheres interconnected to each other by small channels. From insert figure of Fig. 4b, a regularly ordered hexagonal arrangement can be observed and the channels connecting the pores are also clearly observed in each void. The channels correspond to the contact points between the initial polymer spheres and confirm the formation of a 3D framework. It can be seen that the walls of the film were composed by nanoparticles agglomerates, indicating that the framework of the film was constructed by $Cs_{2.5}H_{0.5}PW_{12}O_{40}$ and exhibited self-supported well-ordered 3D structure. The thickness of walls is about 110–130 nm, which can be estimated on the basis of several measurements on SEM images (Fig. 4c). Moreover, the thickness of the porous walls also increased with the times of precursor filtration increasing. The average diameter of the pore size of the $Cs_{2.5}H_{0.5}PW_{12}O_{40}$ film is about 550–600 nm, in which the pore is 10–20% smaller than that of the original PS colloidal spheres (the diameter of the initial PS particles 660 nm Fig. 4a). This result indicated that the $Cs_{2.5}H_{0.5}PW_{12}O_{40}$ composite underwent shrinkage during extraction probably because of the solidifying or restricting the structure of polyoxometalate molecules.

As demonstrated by many group [10,38,39], periodic inverse opal structures exhibit a photonic band stop (PBG), an energy range for which light cannot propagate in any direction inside the crystal, giving them the unique properties of localizing light and controlling spontaneous emission. The position of the stop band can be tuned by adjusting the size of the diameter, so the periodic structure can cover the entire spectra region from visible to near-infrared wavelength range. Although most colloidal crystals or inverse opals with simple structure do not produce an absolute PBG in the visible and near-infrared wavelength range, they show optical stop bands along certain crystal directions, i.e. they only exhibit a pseudo band gap.

The PBG of $Cs_{2.5}H_{0.5}PW_{12}O_{40}$ thin film was also investigated by transmission spectrum. Fig. 5 shows transmittance spectrum collected from $Cs_{2.5}H_{0.5}PW_{12}O_{40}$ inverse opal thin film in air at angle of incidence ($\theta = 0^\circ$). At normal incidence, the $Cs_{2.5}H_{0.5}PW_{12}O_{40}$ inverse opal thin film exhibited a stop band at 1502 nm. Compared to the stop band of PS template at 1425 nm, the stop band of inverse opal $Cs_{2.5}H_{0.5}PW_{12}O_{40}$ thin film was red shift. One reason may be the high refractive index of the $Cs_{2.5}H_{0.5}PW_{12}O_{40}$ nanoparticles [39,40]. In the formation of $Cs_{2.5}H_{0.5}PW_{12}O_{40}$ thin film, increasing the number of layers deposited on the colloidal spheres leads to an increase in both the diameter and the effective refractive index of the spheres, which causes a systematic red shift of the stop bands. The transmission stop band could be controlled in a large region, by the PS's

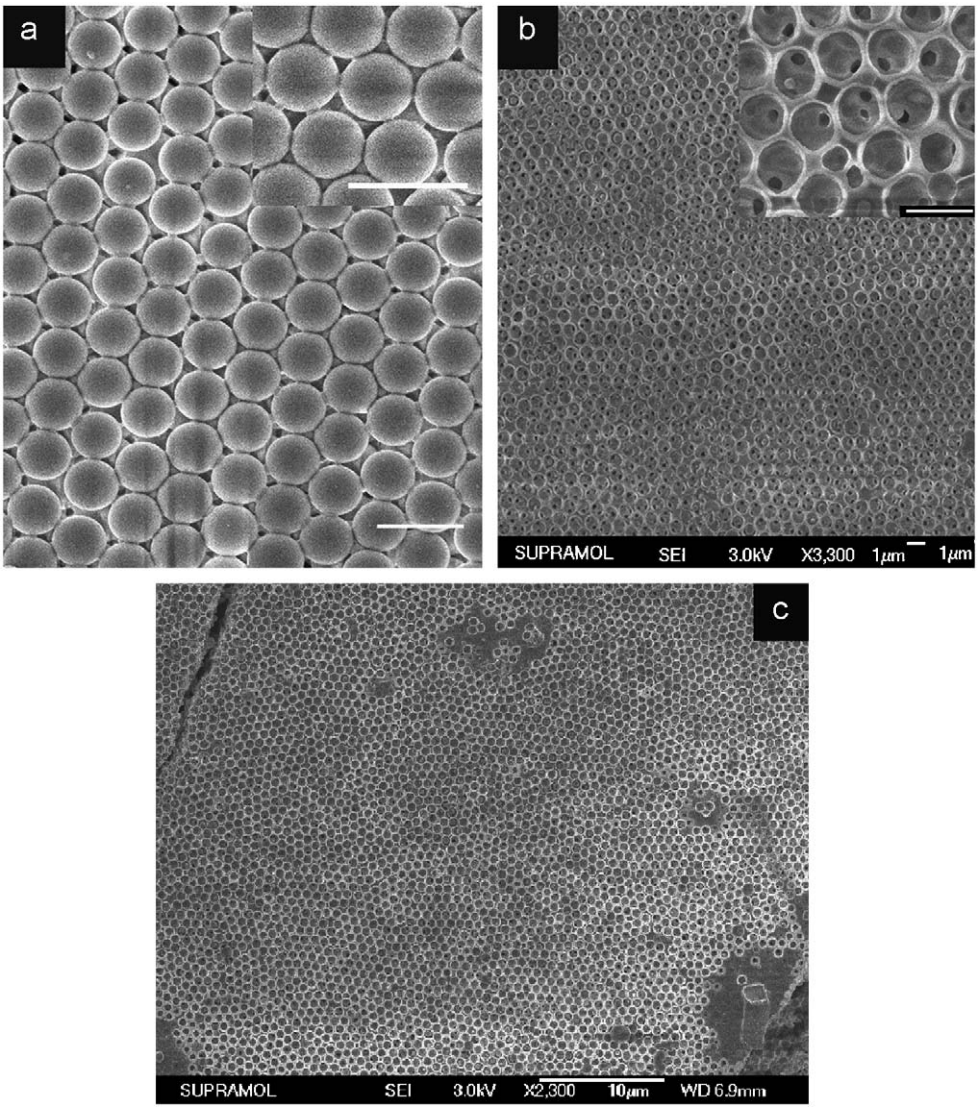

Fig. 4. The SEM images of (a) as-fabricated PS colloidal crystals, (b) $Cs_{2.5}H_{0.5}PW_{12}O_{40}$ thin film after removal of PS template (all scale bars are 1 μm), and (c) the large scale of $Cs_{2.5}H_{0.5}PW_{12}O_{40}$ thin film.

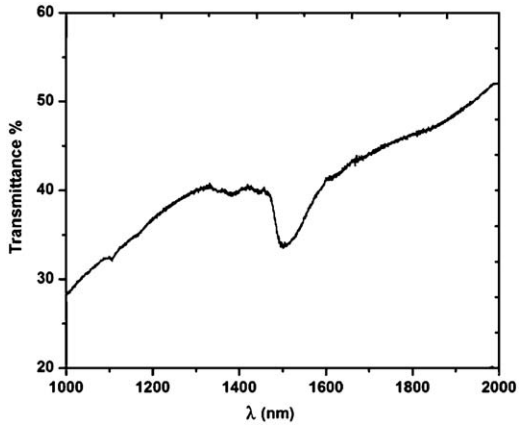

Fig. 5. The transmission spectrum of the $Cs_{2.5}H_{0.5}PW_{12}O_{40}$ film.

size for coarse-tuning, precursor and the deposition time for adjustment [41,42].

The stability of the $Cs_{2.5}H_{0.5}PW_{12}O_{40}$ thin film was also studied. The thin film of $Cs_{2.5}H_{0.5}PW_{12}O_{40}$ would decompose as heating at 550 °C. And in water, the film may be brush off from substrate, but the 3D ordered structure does not change.

4. Conclusion

In summary, 'inverse opal' and 'nanocasting' synthesis of 3D ordered POMs film has been demonstrated for the first time using PS colloidal crystal template. By controlling the infiltration, the ordered 3D array film and ordered porous film fabricated by polyoxometalates can be constructed. The POMs array film displays well-defined array with inverse opal structure. The colloidal crystal template takes some advantages for the synthesis of 3D ordered POMs thin film. In addition, the size of the structures can be well controlled by the colloidal spheres, which will prove to be important in the construction of POMs based thin film with tailored properties. However, there are also some limits, for example, the soluble polyoxometalate could not construct 3D structure by this method. Such a simple method to fabricate POMs inverse opal films with tunable PBG would boost a new application of POMs films in a new generation of optical devices

and catalytic materials, such as high performance reflectors, chemical and biochemical sensors.

Acknowledgments

This work was supported by the National Natural Science Foundation of China (20871026). Supported by analysis and testing foundation of Northeast Normal University and the major projects of Jilin Provincial Science and Technology Department (20060403-4).

Appendix A. Supplementary Materials

Supplementary data associated with this article can be found in the online version at doi:10.1016/j.jssc.2009.03.035.

References

[1] O.D. Velev, A.M. Lenhoff, E.W. Kaler, Science 287 (2000) 2240–2243.
[2] H.Y. Ko, J. Park, H. Shin, Moon, J. Chem. Mater. 16 (2004) 4212–4215.
[3] A.L. Rogach, N.A. Kotov, D.S. Koktysh, J.W. Ostrander, G.A. Ragoisha, Chem. Mater. 12 (2000) 2721–2726.
[4] Y.J. Zhao, X.W. Zhao, C. Sun, J. Li, R. Zhu, Z.Z. Gu, Anal. Chem. 80 (2008) 1598–1605.
[5] H.L. Li, J.X. Wang, L.M. Yang, Y.L. Song, Adv. Funct. Mater. 18 (2008) 1–7.
[6] Y.N. Xia, B. Gates, Y.D. Yin, Y. Lu, Adv. Mater. 12 (2000) 693–713.
[7] G.A. Ozin, S.M. Yang, Adv. Funct. Mater. 11 (2001) 95–104.
[8] Y. Yamauchi, K. Kuroda, Chem. Asian J. 3 (2008) 664–676.
[9] G.Z. Han, Z.Y. Xie, D. Zheng, L.G. Sun, Z.Z. Gu, Appl. Phys. Lett. 91 (2007) 141114.
[10] E. Yablonovitch, Phys. Rev. Lett. 58 (1987) 2059–2062.
[11] J.D. Joannopoulos, P.R. Villeneuve, S.H. Fan, Nature 386 (1997) 143–149.
[12] M. Sadakane, T. Asanuma, J. Kubo, W. Ueda, Chem. Mater. 17 (2005) 3546–3551.
[13] O.D. Velev, T.A. Jede, R.F. Lobo, A.M. Lenhoff, Nature 389 (1997) 447–448.
[14] G. Subramanian, V.N. Manoharan, J.D. Thorne, D.J. Pine, Adv. Mater. 11 (1999) 1261–1265.
[15] O.D. Velev, P.M. Tessier, R.F. Lobo, A.M. Lenhoff, E.W. Kaler, Nature 401 (1999) 548.
[16] X.X. Xu, X. Wang, A. Nisar, X. Liang, J. Zhuang, S. Hu, Y. Zhuang, Adv. Mater. 20 (2008) 3702–3708.
[17] R. Ryoo, S.H. Joo, S. Jun, J. Phys. Chem. B 103 (1999) 7743–7746.
[18] O.V. Branytska, R. Neumann, J. Org. Chem. 68 (2003) 9510–9512.
[19] E. Coronado, M. Clemente–León, J.R. Galán–Mascarós, C. Giménez–Saiz, C.J. Gómez–Garcia, E. Martínez–Ferrero, J. Chem. Soc. Dalton. Trans. 21 (2000) 3955–3961.
[20] M. Green, J. Harries, G. Wakefield, R. Taylor, J. Am. Chem. Soc. 127 (2005) 12812–12813.
[21] L. Gao, E.B. Wang, Z.H. Kang, Y.L. Song, B.D. Mao, L. Xu, J. Phys. Chem. B 109 (2005) 16587–16592.
[22] Y.H. Wang, X.L. Wang, C.W. Hu, J. Colloid Interface Sci. 249 (2002) 307–315.
[23] H.Y. Ma, J. Peng, Z.G. Han, Y.H. Feng, E.B. Wang, Thin Solid Films 446 (2004) 161–166.
[24] T. Yamase, Mol. Eng. 3 (1993) 241–262.
[25] Y.V. Geletii, A. Gueletii, I.A. Weinstock, J. Mol. Catal. A 262 (2007) 59–66.
[26] S.Q. Liu, D. Volkmer, D.G. Kurth, Pure Appl. Chem. 76 (2004) 1847–1867.
[27] M. Xu, C.L. Liu, H.L. Li, W. Li, L.X. Wu, J. Colloid Interface Sci. 323 (2008) 176–181.
[28] T. Ito, H. Yashiro, T. Yamase, Langmuir 22 (2006) 2806–2810.
[29] M. Jiang, X.D. Zhai, M.H. Liu, Langmuir 21 (2005) 11128–11135.
[30] W.F. Bu, H.L. Li, H. Sun, S.Y. Yin, L.X. Wu, J. Am. Chem. Soc. 127 (2005) 8016–8017.
[31] H. Sun, H.L. Li, W.F. Bu, M. Xu, L.X. Wu, J. Phys. Chem. B 110 (2006) 24847–24854.
[32] W. Li, S.Y. Yin, J.F. Wang, L.X. Wu, Chem. Mater. 20 (2008) 514–522.
[33] L.A. Pérez-Maqueda, E. Matijević, Chem. Mater. 10 (1998) 1430–1435.
[34] P. Jiang, J.F. Bertone, K.S. Hwang, V.L. Colvin, Chem. Mater. 11 (1999) 2132–2140.
[35] F. Chai, X.H. Wang, R.X. Tan, F.H. Cao, F.Y. Zhai, L.L. Xu, C.L. Shao, Y.C. Liu, Chem. Lett. 36 (2007) 260–261.
[36] T. Okuhara, H. Watanabe, T. Nishimura, K. Inumaru, M. Misono, Chem. Mater. 12 (2000) 2230–2238.
[37] B. Ding, J. Gong, J. Kim, S. Shiratori, Nanotechnology 16 (2005) 785–790.
[38] R. Mayoral, J. Requena, J.S. Moya, C. LÓpez, A. Cintas, H. Miguez, F. Meseguer, L. Vázquez, M. Holgado, A. Blanco, Adv. Mater. 9 (1997) 257–260.
[39] D.Y. Wang, A.L. Rogach, F. Caruso, Chem. Mater. 15 (2003) 2724–2729.
[40] R.C. Schroden, M. Al-Daous, C.F. Blanford, A. Stein, Chem. Mater. 14 (2002) 3305–3315.
[41] R.C. Schroden, M. Al-Daous, A. Stein, Chem. Mater. 13 (2001) 2945–2950.
[42] J.X. Wang, Y.Q. Wen, H.L. He, Z.W. Zheng, Y.L. Song, L. Jiang, Macromol. Chem. Phys. 207 (2006) 596–604.